

A examination of the temporal evolution of the excited states of DHP and *cis*-stilbene along with some trajectory calculations to test several possible potential energy surfaces may be necessary to unravel the reasons for this. These results suggest that several different microscopic solvent-solute interactions are perturbing the potential energy surface(s) and thereby affecting the excited *cis*-stilbene lifetimes.

**Note Added in Proof.** Repinec et al. (*J. Phys. Chem.* 1991, 95, 10380) have recently reported ultrafast transient absorption

measurements on DHP following *cis*-stilbene excitation. Kinetic modeling of the *cis*-stilbene  $\rightarrow$  DHP reaction suggests an intermediate with a lifetime of  $300 \pm 200$  fs is present. Results from the excitation of DHP are also presented.

**Acknowledgment.** We thank Mr. Chris Dries for technical assistance and the Office of Naval Research for support of this research through the Naval Research Laboratory.

Registry No. (Z)-Stilbene, 645-49-8.

## Redox Properties of Small Semiconductor Particles

Naomi Liver and Abraham Nitzan\*

School of Chemistry, The Sackler Faculty of Science, Tel Aviv University, Tel Aviv 69978, Israel  
(Received: June 24, 1991; In Final Form: November 8, 1991)

In this paper we study the equilibrium properties of semiconductor particles of intermediate sizes ( $\geq$  Debye length) in contact with an electrolyte solution containing a given redox pair. We focus on the size dependence of electrical and thermodynamical quantities associated with such particles. The equilibrium distribution of the potential and of the charge in the particle and in the surrounding electrolyte is obtained analytically in limiting cases and computed in the general case using the nonlinear Poisson-Boltzmann equation, assuming Boltzmann statistics for carrier distributions in the semiconductor. A simple relation for the size-dependent redox potential of a semiconductor sphere characterized by its radius and charge is proposed and is found to provide a good approximation for a broad range of electrolyte concentrations. This leads to an expression for the "equilibrium constant" for the semiconductor/electrolyte system, which relates the concentrations of the electrolytic redox components to the concentration, size, and charge of the semiconductor particles.

### I. Introduction

The physical and chemical properties of small particles and clusters have been subjects of many studies over the last decade.<sup>1-6</sup> A common feature to many of these studies is the generic question concerning the size evolution of macroscopic bulk properties. Of particular interest for potential applications are such size-dependent properties which imply unique chemical or photochemical activity of small clusters. The observation of unique size-dependent photochemical activity in colloidal semiconductor particles has led to intense research, mostly motivated by the need to develop efficient photochemical processes for solar energy conversion.<sup>7-10</sup> Such processes involve redox reactions which follow the photogeneration of nonequilibrium concentrations of electrons and holes in the semiconductor. Consequently, the question of the size dependence of the redox potential naturally arises.<sup>10-12</sup> It should be emphasized, however, that such photoredox reactions, being

inherently nonequilibrium processes, are not directly related to the equilibrium redox potential of a suspension of semiconductor particles.

In the present paper we focus on the equilibrium redox properties of well-characterized semiconductor particles in the dark. Our results are therefore not directly related to the photoredox properties of these systems, but to the question of size evolution of macroscopic, in the present case surface, properties. The model semiconductor particles are assumed to be spheres. The semiconductor is characterized by its macroscopic bulk and surface properties: the band gap, the absolute positions of the band edges and of the Fermi energy, and the density and nature of the dopants. We investigate the redox properties of such particles by studying their equilibrium with an electrolyte solution containing a given redox pair.

Previous work on particle size dependence of redox properties has focuses on small metal particles.<sup>13-16</sup> The equilibrium  $M \rightleftharpoons M^{++}(\text{aq})$  between a metal M and its solvated ion in water depends on the state of the metal. For example, the case where M is M(aq) (dispersed metal atoms) and the case where M is a bulk metal electrode differ in their free energies by the sum of the free energies of dispersion and hydration (per atom) of the bulk metal. Henglein<sup>12a</sup> has shown that for silver atoms this implies a standard redox potential for the Ag/Ag<sup>+</sup> of  $\sim -1.8$  V, as opposed to +0.8 V for the same equilibrium with a silver electrode. Plieth<sup>13</sup> has derived a relation for the size dependence of the redox potential associated with the M(cluster)/M<sup>+</sup>(aq) equilibrium into which the size dependence enters via the surface tension of the metal-

(1) See papers cited in the proceedings of The International Symposium on Small Particles and Clusters. *Z. Phys.* 1989, D12.

(2) Halperin, W. P. *Rev. Mod. Phys.* 1986, 58, 533.

(3) Benedek, G., Martin, T. P., Pacchioni, G., Eds. *Elements and Molecular Clusters*; Springer: Berlin, 1988.

(4) Henglein, A. *Pure Appl. Chem.* 1984, 56, 1215.

(5) Moser, J.; Grätzel, M. *J. Am. Chem. Soc.* 1983, 105, 6547.

(6) Fox, M. A.; Lindig, B.; Chen, C. C. *J. Am. Chem. Soc.* 1982, 104, 5828.

(7) Bard, A. J. *Ber. Bunsenges. Phys. Chem.* 1988, 92, 1187.

(8) Grätzel, M. *Ber. Bunsenges. Phys. Chem.* 1980, 84, 981.

(9) Heller, A. *Acc. Chem. Res.* 1981, 14, 154.

(10) Brus, L. E. *J. Phys. Chem.* 1986, 90, 2555.

(11) (a) Brus, L. E. *J. Phys. Chem.* 1984, 80, 4403. (b) Rossetti, R.; Beck, S. M.; Brus, L. E. *J. Am. Chem. Soc.* 1984, 106, 980.

(12) (a) Henglein, A. *Ber. Bunsenges. Phys. Chem.* 1977, 81, 556. (b) Fojtik, A.; Weller, H.; Koch, U.; Henglein, A. *Ber. Bunsenges. Phys. Chem.* 1984, 88, 969. (c) Weller, H.; Koch, U.; Gutierrez, M.; Henglein, A. *Ibid.* 1984, 88, 649.

(13) Plieth, W. J. *J. Phys. Chem.* 1982, 86, 3166.

(14) Horanyi, G. *J. Phys. Chem.* 1985, 89, 2967.

(15) Konstantinov, I.; Panov, A.; Malinowski, J. J. *Photogr. Sci.* 1973, 21, 250.

(16) Konstantinov, I.; Malinowski, J. J. *Photogr. Sci.* 1975, 23, 1.

/water interface, in analogy to the Kelvin equation for the size dependence of the vapor pressure above a liquid droplet. Note that in the equilibria considered in these examples the metals participate chemically in the process considered. Another possibility is that the metal particles only act as suppliers or absorbers of electrons (the case where M is solvated neutral metal atom corresponds to both cases). The processes discussed in the present work are of the second type: the semiconductor particles are assumed to enter the redox process only by exchanging electrons with the electrolyte solution.

The semiconductor particles considered in the present work are relatively big, of the order of the Debye length (a few hundred angstroms at the carrier density ranges considered) and larger. Very small semiconductor particles cannot be characterized by the corresponding bulk properties. Thus a dopant density of  $10^{18} \text{ cm}^{-3}$  corresponds to an average of 0.5 dopant particles per sphere of radius 50 Å. For such small clusters, the statistical distribution of semiconductor particles with different number of dopants, rather than the mean properties for a given density of dopants, is dominant. Also, we use the Poisson-Boltzmann (PB) equation in order to analyze the chemical and electrostatic equilibrium between the semiconductor and the electrolyte solution, in analogy to the procedure used for the bulk semiconductor-electrolyte interface.<sup>17</sup> This is essentially a mean field theory which breaks down if the number of charge carriers is too small. Thus, the results presented in the present paper are not directly valid for very small (a few nanometers) particles; however, they should describe well the behavior of particles of size  $\geq$  Debye length, and in particular, the size evolution from the small particle limit to the macroscopic surface.

The semiconductor sphere model has been discussed before by several authors. Brus<sup>10</sup> has considered this model in the limit of very small particles, focusing on the quantum states of electrons and electron-hole pairs in spherical dielectric particles. A similar treatment has been put forward by Henglein and co-workers.<sup>12</sup> These discussions of electronic states in confined dielectric environments have served to explain the observed size-dependent blue shifts in exciton absorption in nanometer size colloidal semiconductor particles relative to the bulk materials. More closely related to the present paper are the works by Albery and co-workers<sup>18</sup> who have treated a spherical semiconductor particle in the total depletion limit, and, also for a depletion case, in the very large sphere limit. These authors focus on the potential distribution within the particle as a necessary input for a discussion of carrier transport in the particle. We focus on the size evolution of redox properties, for which we require an exact solution of the PB equation describing the particle-electrolyte solution.

The description of equilibrium between a macroscopic flat semiconductor electrode and an electrolyte solution containing a given redox pair<sup>17</sup> is achieved by equating the electrochemical potentials of electrons in the two phases. In the semiconductor this is determined by the Fermi energy and in the electrolyte—by the redox potential which depends on the relative concentrations of the redox pair. When a semiconductor flat electrode is replaced by a distribution of small colloidal particles, two new characteristic properties of the semiconductor system emerge: the concentration of the particles and their size (or size distribution). The description of equilibrium in such a system has to be expressed also in terms of these quantities. In a sense, a semiconductor particle plays now the same role as one of the ions in the electrolyte solution. The main difference lies in the fact that such a particle can be in many "oxidation states", characterized by the number of electrons that it gains from or gives to the electrolyte. In principle the redox potential (Fermi energy) of the semiconductor is related to the relative equilibrium concentrations of all these states. For the large particles considered here, for which the average numbers

of electrons exchanged with the electrolyte can be several hundreds or thousands, it is more useful to use the Fermi energy of the particle. The latter may in turn be expressed in terms of the number of electrons gained or lost by the particle and of the particle size. The basic question of chemical equilibrium is: Given the nature and the initial concentrations of the reactants, what are the concentrations of reactants and products at the final equilibrium state? This may be answered by considering the charge exchange balance between the semiconductor particles and the electrolyte. The result depends on the density and size of the semiconductor particles.

While the above considerations and the main focus of the paper are related to the semiconductor electrolyte equilibrium in the dark, they have direct bearings on the optical properties, and hence on the photochemical activity of semiconductor particles under such equilibrium conditions. Liu and Bard<sup>19</sup> have recently discussed the implications of charging a semiconductor particles on the shift in the absorption band edge. The origin of this shift (first discussed by Burstein<sup>20</sup>) lies in the fact that the absorption probability depends on the electronic levels occupation numbers via factors like  $f_v(1 - f_c)$ , where  $f_v$  and  $f_c$  are occupation numbers for levels in the valence and conduction bands, respectively. For semiconductor particles at equilibrium with an electrolytic redox pair these occupation numbers change, leading to a shift in the absorption edge which depends on the redox potential in the solution. This suggests a potentially very useful way to monitor the semiconductor particles/electrolyte equilibrium. The implications for photoelectrochemistry are obvious.

In this paper we limit our discussion to ideal semiconductor particles which do not contain surface states, and which therefore may be considered as finite spheres of bulk material. The effect of surface states will be considered in a subsequent paper. In section II we describe in detail the equilibrium between a single spherical semiconductor particle and an electrolyte solution, and in section III we discuss the dependence of the redox potential or the Fermi energy of a particle on its size, charge, and the surrounding redox system. The equilibrium between a finite density of colloidal SC particle and an electrolytic redox system is discussed in section IV.

## II. The Semiconductor Sphere-Electrolyte Equilibrium

In this section we consider a spherical semiconductor (SC) particle of radius  $R$  embedded in an electrolyte solution. To analyze the equilibrium between the two systems we have to evaluate the potential and charge distributions in each of them. We first consider the spherical particle and as a reference point we take the potential in the bulk of the electrolyte to be zero. The SC is assumed to be nondegenerate so that the local concentrations  $p(r)$  and  $n(r)$  of holes and electrons are assumed to obey Boltzmann statistics. Furthermore, the impurity atoms (donors and acceptors) are assumed to be fully ionized. Under these assumptions the space charge density is given by

$$\rho = q[(p - p_b) - (n - n_b)] \quad (1)$$

where  $q$  denotes the electron charge and where  $p = p(r)$  and  $n = n(r)$  are the local concentrations of holes and electrons, respectively, while  $p_b$  and  $n_b$  are the corresponding quantities in the interior of a macroscopic ( $R \rightarrow \infty$ ) bulk semiconductor (we assume that the intrinsic carrier densities are negligible relative to the impurity originated ones, so that  $p_b = N_A$ ,  $n_b = N_D$ , where  $N_A$  and  $N_D$  are the densities of acceptors and donors, respectively).  $p(r)$  and  $n(r)$  satisfy

$$\begin{aligned} p(r) &= p_b e^{-\beta q(\phi(r) - \phi_b)} \\ n(r) &= n_b e^{\beta q(\phi(r) - \phi_b)} \end{aligned} \quad (2)$$

where  $\phi(r)$  is the local potential in the SC sphere and  $\phi_b$  is the fully developed equilibrium potential difference between the interior of a macroscopic bulk semiconductor and the electrolyte.

(17) Pleskov, Y. V.; Gurevich, Y. Y. *Semiconductor Photo Electrochemistry*; Consultants Bureau: New York, 1986.

(18) (a) Albery, W. J.; Bartlett, P. N. *J. Electrochem. Soc.* **1984**, *131*, 315. (b) Albery, W. J.; Bartlett, P. N.; Porter, J. D. *J. Electrochem. Soc.* **1984**, *131*, 2892. (c) Albery, W. J.; Bartlett, P. N.; Porter, J. D. *J. Electrochem. Soc.* **1984**, *131*, 2896.

(19) Liu, C.; Bard, A. J. *J. Phys. Chem.* **1989**, *93*, 3232.

(20) Burstein, E. *Phys. Rev.* **1954**, *93*, 632.

$\phi_b$  is therefore the difference between the original position of the Fermi level of the SC and that of the electrolyte. The latter is the redox potential of the electrolyte system expressed on the vacuum scale.

The electrostatic potential  $\phi$  is the solution, with appropriate boundary conditions, of the Poisson equation

$$\nabla^2 \phi = -\frac{4\pi}{\epsilon_{SC}} \rho(r) \quad (3)$$

where  $\epsilon_{SC}$  is the static dielectric constant of the SC. Equations 1–3 lead to the Poisson–Boltzmann equation, which for the present case of spherical symmetry takes the form

$$\frac{d^2 \Phi}{dr^2} + \frac{2}{r} \frac{d\Phi}{dr} = \frac{1}{L_{SC}^2} [A(1 - e^{-\Phi}) + B(e^{\Phi} - 1)] \quad (4)$$

where

$$\Phi = \beta q(\phi - \phi_b) \quad (5a)$$

is the dimensionless potential,

$$A = \frac{p_b}{p_b + n_b} \quad B = \frac{n_b}{p_b + n_b} \quad (5b)$$

are intrinsic properties of the semiconductor, and

$$L_{SC} = \left[ \frac{\epsilon_{SC}}{4\pi q^2 \beta (n_b + p_b)} \right]^{1/2} \quad (5c)$$

is the Debye length in the SC. The boundary conditions for eq 4 are

$$\left. \frac{d\Phi}{dr} \right|_{r=0} = 0 \quad (6a)$$

$$\Phi(R) = \Phi_R \quad (6b)$$

Equation 6a results from symmetry considerations. Equation 6b introduces the potential at the sphere surface as a parameter to be considered later.

Equation 4 cannot be solved analytically in its general form. Analytic solutions are known for some limiting cases: (a) If  $0 < |\Phi| \ll 1$  throughout the particle, eq 4 may be linearized, leading to

$$\Phi(r) = \Phi_R \frac{R}{r} \frac{\sinh(r/L_{SC})}{\sinh(R/L_{SC})} \quad (7)$$

In this limit, the field at the sphere surface and the net charge in the particle are given by

$$Q_{SC} = \epsilon_{SC}(\phi_R - \phi_b) R^2 \left[ \frac{1}{R} - \frac{1}{L_{SC}} \frac{\cosh(R/L_{SC})}{\sinh(R/L_{SC})} \right] = \epsilon_{SC} R^2 E_{SC} \quad (8)$$

(b) In the case of a heavily doped small n-type (p-type) semiconductor particle with a negative (positive) surface potential, large enough so that the particle is entirely depleted of its majority carriers, but not too large so the Fermi energy is still far from the band edges, eq 4 becomes<sup>18a</sup> (for the specific example of an n-type SC)

$$\frac{d^2 \Phi}{dr^2} + \frac{2}{r} \frac{d\Phi}{dr} = -\frac{1}{L_{SC}^2} \quad (9)$$

whose solution is

$$\Phi = \Phi_0 - \frac{1}{6} \left[ \frac{r}{L_{SC}} \right]^2 \quad (10)$$

where  $\Phi_0 = \Phi_R + R^2/6L_{SC}^2$  is the potential at the center.

For the general case, eq 4 can be solved numerically to yield the potential distribution and the charge accumulation in the SC

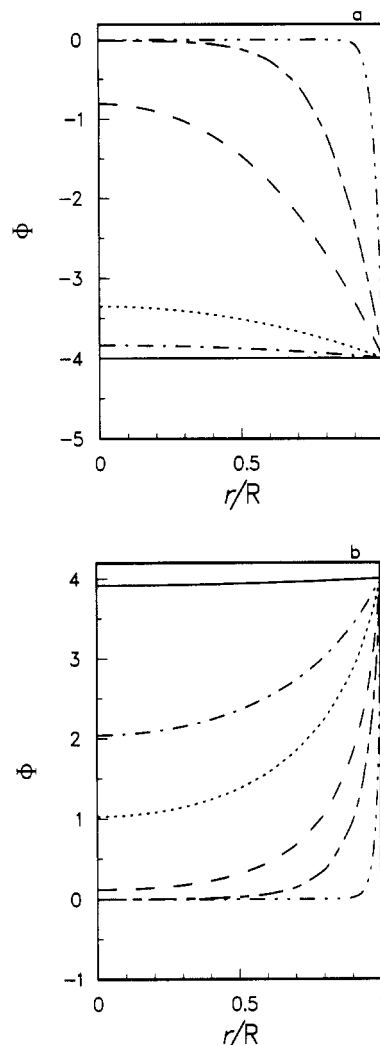


**Figure 1.** The dimensionless potential  $\Phi$  in the SC sphere as a function of the ratio between the sphere center and its radius for different sphere sizes. Surface potential is  $-4$  in Figure 1a and  $+4$  in Figure 1b. (—)  $R_D = 0.1L$ ; (---)  $R = 1L_D$ ; (· · ·)  $R = 2L_D$ ; (- · - ·)  $R = 5L_D$ ; (- - -)  $R = 10L_D$ ; (- · - · - ·)  $R = 50L_D$ . The latter case is indistinguishable from a planar SC.

particle. In many situations we will encounter special cases of eq 4. For an intrinsic SC ( $n_b = p_b = n_i$ ) eq 4 becomes

$$\frac{d^2 \Phi}{dr^2} + \frac{2}{r} \frac{d\Phi}{dr} = \frac{1}{(L_{SC}')^2} (e^{\Phi} - e^{-\Phi}) \quad (11)$$

where

$$(L_{SC}')^2 = \frac{\epsilon_{SC}}{4\pi q^2 \beta n_i} \quad (12)$$

For an n-type wide band gap SC where  $N_D \gg n_i, N_A$  and where  $n_b \approx N_D \gg p_b$ , eq 4 becomes

$$\frac{d^2 \Phi}{dr^2} + \frac{2}{r} \frac{d\Phi}{dr} = \frac{1}{L_{SC}^2} (e^{\Phi} - 1) \quad (13)$$

Similarly, for p-type SC where  $N_A \gg n_i, N_D$  and where  $p_b \approx N_A \gg n_b$

$$\frac{d^2 \Phi}{dr^2} + \frac{2}{r} \frac{d\Phi}{dr} = \frac{1}{L_{SC}^2} (1 - e^{-\Phi}) \quad (14)$$

It should be kept in mind that  $\Phi$  is to be determined by fitting to the electrolyte side of the interface.

Before considering the electrolyte side, we show in Figures 1–3 some results which demonstrate the effect of the finite particle size on the potential distribution and the charge in the SC particle. In these figures  $\Phi_R$ , the difference between the surface potential

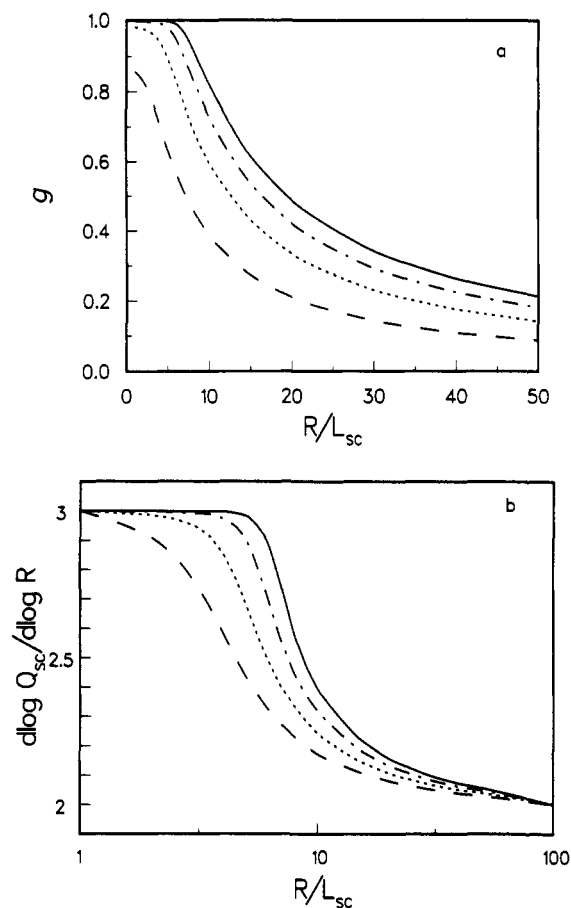


**Figure 2.** (a) The charge density  $g = Q_{sc}/qVN_d$  ( $V$ , particle volume) as a function of  $R$  for different negative surface potentials (depletion). (b) The same data plotted as  $d[\log Q_{sc}]/d[\log R]$  vs  $[R/L_{sc}]$ . Full line:  $\Phi_R = -8$ ; dashed-dotted line:  $\Phi_R = -6$ ; dotted line:  $\Phi_R = -4$ ; dashed line:  $\Phi_R = -2$ .

and the potential that would have existed in the interior of the particle in the limit  $R \rightarrow \infty$ , is used as a parameter. The SC is taken to be n-type wide bandgap material, so eq 13 has been used to compute  $\Phi$ .

Figure 1a shows, for  $\Phi_R = -4$ , the potential distribution in the particle for different particle sizes. Figure 1b shows similar results for  $\Phi_R = 4$ . It is seen that for  $R \leq L_{sc}$  the potential is almost constant and the bands are unbent throughout the particle. The same is true for  $R \rightarrow \infty$ , except in the space charge region of order  $L_{sc}$  near the surface.

Figures 2 and 3 show the charge in the particle as a function of  $\Phi_R$  for particles of different sizes. In Figure 2a,b we show the charge in the SC particle as a function of its size  $R$ , for several negative values (depletion) of  $\Phi_R$ . In these figures the same data is shown: In Figure 2a we plot the charge per unit volume ( $g = Q_{sc}/qVN_d$ ;  $V = 4\pi R^3/3$ ) as a function of the sphere size. For  $R \rightarrow \infty$ ,  $g \sim 1/R$ , reflecting the fact that the accumulated charge is proportional to the particle surface area. Figure 2b shows the size dependence of the slope  $d(\log Q_{sc})/d \log R$ . This slope changes from 3 at small  $R$ , where the charge is proportional to the particle volume, to 2 as  $R \rightarrow \infty$ , again reflecting the surface nature of the charging in this limit. In Figure 3a,b we show similar results for the case of accumulation ( $\Phi_R > 0$ ). Note that in this case the slope of  $\log Q_{sc}$  vs  $\log R$  approaches the value 3 as  $R/L_{sc} \rightarrow 0$  much more slowly than in the depletion case. In the latter, when conduction band electrons are depleted from the SC particle,  $g \rightarrow 1$  when  $\Phi_R \rightarrow -\infty$  (see Figure 2a). Such an upper limit on  $|g|$  does not exist in the case of  $\Phi_R > 0$  (Figure 3a) where electrons enter the semiconductor. Here the charge density can be much larger for the same  $|\Phi_R|$  and the proportionality to the volume is approached more slowly when  $R \rightarrow 0$ .

Next consider the electrolyte side. We use the Gouy-Chapman theory<sup>21</sup> for the description of the ionic part of the double layer.

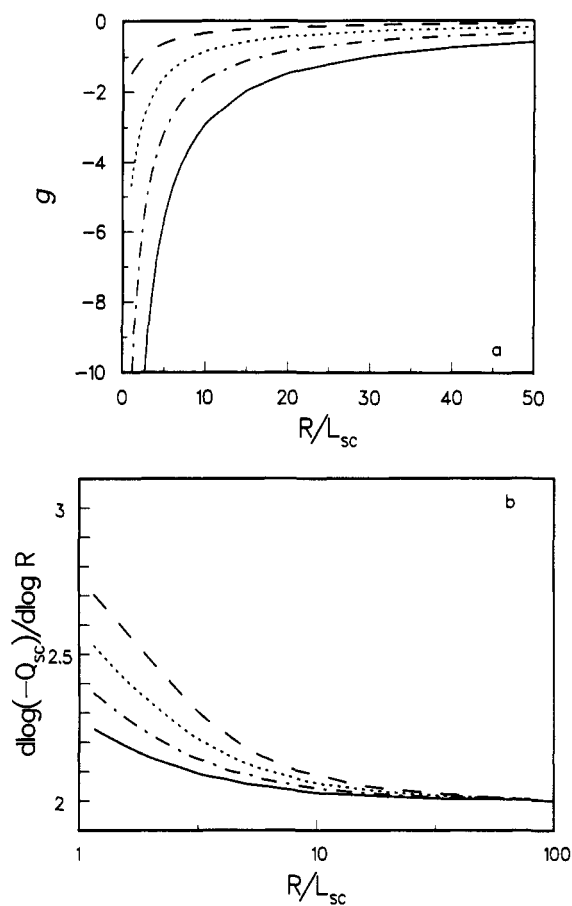


**Figure 3.** Same as Figure 2, for positive values of  $\Phi_R$  (accumulation): full line,  $\Phi_R = 4$ ; dashed-dotted line,  $\Phi_R = 3$ ; dotted line,  $\Phi_R = 2$ ; dashed line,  $\Phi_R = 1$ .

This theory is based on the Poisson-Boltzmann equation which now takes the form

$$\frac{1}{r} \frac{d^2 r \phi}{dr^2} = -\frac{4\pi}{\epsilon_{el}} \rho(r) \quad (15)$$

$$\rho(r) = q \sum_i Z_i c_i^+(r) - q \sum_i Z_i c_i^-(r) \quad (16)$$

where  $\epsilon_{el}$  is the dielectric constant of the solution ( $\sim 80$  for water),  $Z_i$  are the ionic charge numbers, and

$$c_i^+(r) = c_i^{0+} e^{-Z_i \beta q \phi(r)} \\ c_i^-(r) = c_i^{0-} e^{Z_i \beta q \phi(r)} \quad (17)$$

The potential in the bulk of the electrolyte is set by our choice to be zero.  $c_i^{0+}$ ,  $c_i^{0-}$  are the concentrations of the ions in the bulk of the solution (namely far from the SC particle). They are related by the condition of electroneutrality.

$$\sum_i Z_i c_i^{0+} = \sum_i Z_i c_i^{0-} \quad (18)$$

where the sum over  $i$  goes over all ion types in the solution. They also determine the Debye length of the electrolyte

$$L_{el} = \left[ \frac{\epsilon_{el}}{4\pi q^2 \beta \sum_i Z_i^2 c_i^{0-}} \right]^{1/2} \quad (19)$$

Again, analytical solution may be obtained only in the linear case, ( $\beta q \phi(r) \ll 1$ ). In this limit

$$\Phi_{el}(r) = \Phi_G \frac{R}{r} \exp\left(-\frac{r-R}{L_{el}}\right) \quad (20)$$

(21) Bockris, J. O'M.; Reddy, A. K. V. *Modern Electrochemistry*; Plenum Press: New York, 1970.

where  $\Phi_{el}(r) = \beta q \phi(r)$  and  $\Phi_G = \beta q \phi_G$ .  $\phi_G$  is the potential at the SC side of the Gouy layer. The electric field at the surface and the total charge in the Gouy layer are given in this limit by

$$Q_{el} = -\epsilon_{el} R \left( \frac{R}{L_{el}} + 1 \right) \phi_G = -\epsilon_{el} R^2 E_{el} \quad (21)$$

A complete solution of the SC particle–electrolyte solution equilibrium is obtained by matching the numerical solutions of eq 4 (or one of its variants (11), (13), or (14)) and the equation resulting from eqs 15–17. These are two second-order differential equations, and four boundary conditions are needed to specify a unique solution. These are (1)  $d\Phi/dr = 0$  at  $r = 0$  (the center of the SC sphere); (2)  $\Phi(r \rightarrow \infty) = 0$  (in the interior of the electrolyte); (3) overall charge neutrality in the system:  $Q_{SC} = -Q_{el}$ ,<sup>22</sup> and (4) continuity of the potential across the interface. In addition, the constant  $\phi_b$ , the potential in the interior of a bulk semiconductor in equilibrium with the same electrolyte, is determined from

$$q\phi_b = E_{F,SC}^0 - E_{F,el} \quad (22)$$

where  $E_{F,SC}^0$  is the Fermi energy of the free semiconductor. For example, for an n-type SC with fully ionized donors it is given by

$$E_{F,SC}^0 = E_c - kT \ln [N_C/N_D] \quad (23)$$

where  $E_c$ ,  $N_C$ , and  $N_D$  are the conduction band edge energy, the density of states in the conduction band, and the donor density, respectively.  $E_{F,el}$  is the Fermi energy of the electrolyte

$$E_{F,el} = -q\Phi_{ox|red} + C \quad (24)$$

$\Phi_{ox|red}$  is the redox potential of the electrolyte relative to the standard  $H_2/H^+$  electrode (SHE)

$$\Phi_{ox|red} = \Phi_{ox|red}^0 + \frac{kT}{nq} \ln \frac{c_{ox}}{c_{red}} \quad (25)$$

$q$  is the electron charge,  $n$  is the number of electron transferred in the redox process, and  $C$  is the difference between this electrochemical scale and the physical (vacuum) scale.  $C$  is estimated to be 4.2–4.8 eV.<sup>23</sup> In the calculations described below we took  $C = 4.5$  eV. Note that in eq 25  $c_{ox}$  and  $c_{red}$  represent in general products of concentrations corresponding to the particular redox system.

In order to use the continuity of the potential across the interface we need to take into account the potential drop across the Helmholtz layer associated with the discrete structure of the electrolyte on the atomic scale. To this end we assume that the Helmholtz layer (with width  $\sim$  ionic diameter) does not depend on the particle size. Its electrical properties can therefore be inferred from bulk measurements of its capacity. Denoting by  $E_H$  the electric field in the Helmholtz layer,  $\epsilon_H$  its dielectric constant, and  $d_H$  its width, we have for the potential drop across the Helmholtz layer

$$\phi_H = E_H d_H = \epsilon_{SC} E_{SC}(R) \frac{d_H}{\epsilon_H} = \frac{\epsilon_{SC} E_{SC}(R)}{4\pi C_H} \quad (26)$$

where  $E_{SC}(R)$  is the electric field at the particle surface and  $C_H$  is the differential capacity of the Helmholtz layer. Its experimentally determined value is of the order<sup>24</sup> 6–8  $\mu\text{F}/\text{cm}^2$ . In the calculations presented below we took the value  $C = 8 \mu\text{F}/\text{cm}^2$ .

With these model assumptions we can now calculate the potential distribution and the charge for a given spherical SC particle embedded in an electrolyte solution as a function of its size, the

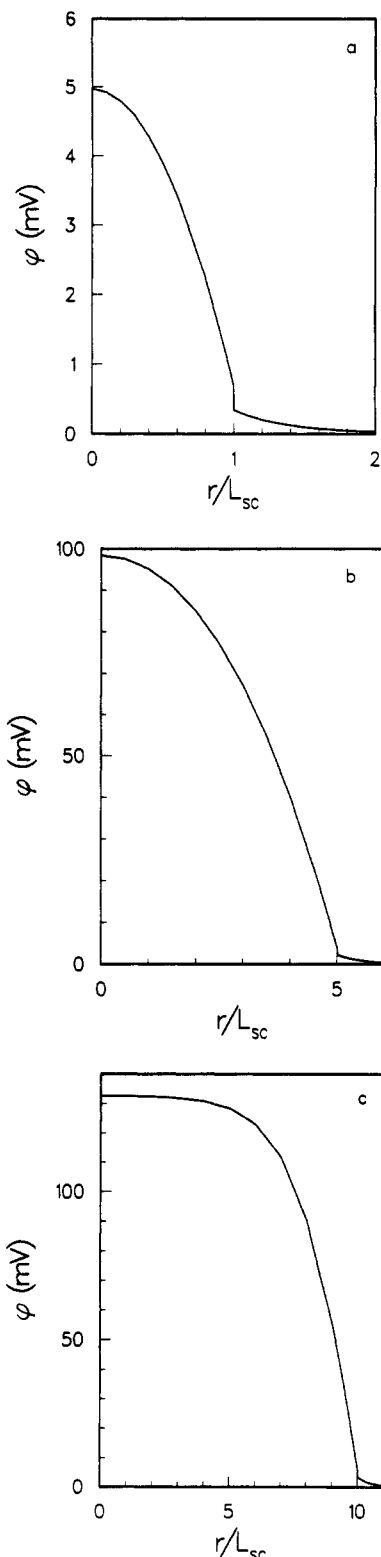


**Figure 4.** Potential profile (as a function of  $r$ , the distance from the particle center) in a system of CdS sphere in methylviologen redox solution. Parameters used for the SC particle and for the electrolyte are given in the text. (a)  $R = L_{SC}$ ; (b)  $R = 5L_{SC}$ ; (c)  $R = 10L_{SC}$ .

characteristics of the bulk semiconductor (band structure, impurities, carrier densities), and the type and concentration of the electrolyte solution. The potential difference between the center of the particle and the interior of the electrolyte solution is given as a sum of the different contributions (SC space charge layer, and Helmholtz and Gouy potentials) which are determined as described above.

The numerical solution of the PB equation was obtained using the DVCPR routine of the IMSL library. The two numerical

(22) Note that the condition  $Q_{SC} = -Q_{el}$  together with  $E(R) = -(4\pi/\epsilon)\sigma$ , where the surface charge is  $\sigma = Q/4\pi R^2$ , implies  $\epsilon_{SC} E_{SC}(R) = \epsilon_{el} E_{el}(R)$ , so this electrostatic condition is not an additional boundary condition.

(23) See for example, ref 17, p 61.

(24) Myamlin, V. A.; Pleskov, Y. V. *Electrochemistry of Semiconductors*; Plenum Press: New York, 1967.

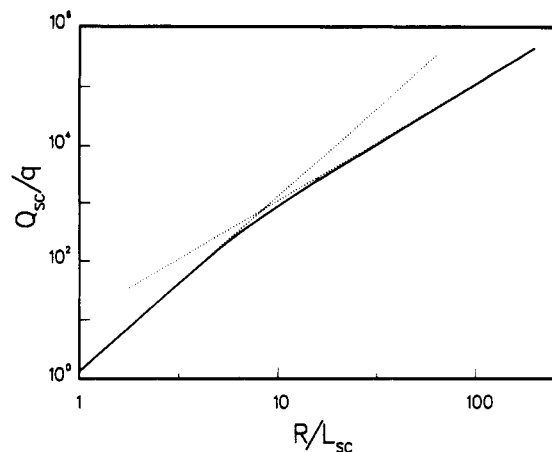


**Figure 5.** The charge accumulated on a CdS particle as a function of its size. Note the change of slope  $d(\log Q_{SC})/d(\log R)$  (indicated by the dashed lines) from 3 for  $R \leq L_{SC}$  to 2 for  $R \gg L_{SC}$ .

nonlinear algebraic equations which represent the boundary conditions were solved using ICSSCU and ICSEVU routines for spline interpolation and the ZSPOW routine for solving the equations.

Figures 4 and 5 show results of numerical calculations on CdS particles in methylviologen  $Mv^+/Mv^{2+}$  electrolyte solution at 300 K. CdS is a wide band gap n-type semiconductor whose gap width is 2.4 eV and its static dielectric constant is 8.9. For the density of the donors we take, unless otherwise stated, the typical value  $2 \times 10^{16} \text{ cm}^{-3}$ . For this donor density (with all the donors assumed ionized) the Debye length  $L_{SC}$  is 252 Å. The Fermi level of the (bulk) SC is 0.122 eV below the conduction band edge and 0.578 eV above the Fermi level of the SHE (i.e., C of eq 24). The standard (SHE)  $Mv^+/Mv^{2+}$  redox potential is  $-0.445 \text{ eV}$ . The electrolyte concentration ( $Mv^+ + Mv^{2+}$ ) was taken  $1.66 \times 10^{-4} \text{ M}$  (i.e.,  $1 \times 10^{17} \text{ ions/cm}^3$ ) and for the particular examples shown here we used  $c_{Mv^+} = c_{Mv^{2+}}$ , so the Fermi level of this solution is 0.445 eV above that of the SHE. Thus  $\phi_b = 0.133 \text{ eV}$ . The charge of the counter ions is taken as  $-2$  and their concentration is  $7.5 \times 10^{16} \text{ cm}^{-3}$ . The Debye length calculated from eq 19 is  $L_{el} = 145 \text{ Å}$ .

Under these conditions the absolute value of the potential drop in the SC is much larger than the absolute value of the Helmholtz potential and of the potential drop in the solution, and consequently, the main part of the interfacial potential drop lies in the space charge region of the semiconductor. Since the Fermi level of the bulk SC is higher than that of the electrolyte solution, electrons go out of the semiconductor and a depletion layer is formed at equilibrium. In Figure 4a–c we show the potential profile in this system for different sizes ( $R/L_{SC} = 1, 5, 10$ ) of the SC particles. For small particles ( $R \leq L_{SC}$ ) the band bending in the particle is small. When  $R \geq 10L_{SC}$  the particle is nearly in the bulk limit and the potential reaches the bulk value ( $\phi_b \approx 133 \text{ mV}$ ) at the sphere center. Figure 5 depicts the (positive) charge accumulated on the SC particle as a function of its radius. It is seen that the charge changes by 3 orders of magnitudes when the particle size varies between  $R = 1L_{SC}$  to  $10L_{SC}$ . As before (Figure 2b) the slope of the  $Q_{SC}$  vs  $R$  plot changes from nearly 3 at for  $R \leq L_{SC}$  to 2 for  $R \gg L_{SC}$ , indicating the transition from volume to surface charging as the sphere size increases.

### III. The Redox Potential of a Colloidal Semiconductor Particle

The oxidation reduction properties of an electrolyte system containing a redox pair with concentrations  $c_{red}$  and  $c_{ox}$  are characterized by the redox potential given by eq 25.  $\Phi_{ox/red}$  measures the tendency of the redox system to exchange electrons with another system.

What is the equivalent property in a dispersion of SC particles? Consider a finite density  $c_{SC}$  of semiconductor particles, which for simplicity we take to be of uniform size. We assume that this density is low enough so that direct interparticle interactions can

be neglected. This is equivalent to the assumption of low concentration in the electrolyte solution which makes it possible to approximate activities by concentrations in eq 25. Under this assumption  $\Phi_{ox/red}$  does not depend on the absolute concentrations of the redox components, only on their ratio.

If we want to treat the SC particles (P's) in complete analogy to this electrolyte system, we should consider all the oxidation states  $P^z$  of one particle, and all the equilibrium reactions  $P^z + e^- \rightleftharpoons P^{z-1}$ . For a simple n-type SC with all the donors ionized,  $z$  can take values from  $N_D V$  to  $-(N_C - N_D)V$ , where  $N_C$  is the density of states in the conduction band (the electrolytic redox pair corresponds to the case where  $z$  can take only two values). The redox properties of the colloid could be calculated in principle in terms of the distribution of particles along these states.

A different point of view is reached by coming down from the macroscopic limit. For a macroscopic SC the Fermi energy (which is equivalent to the redox potential, cf eq 24) is an intrinsic property, determined by its electronic structure and its surface potential and independent of the particle density. This should remain true for a finite size particle, at least when it is large enough. However, the Fermi energy should now depend, in addition to the properties of the macroscopic SC, also on the particle size.

The fact that the redox properties of a dispersion of SC particles may be associated either with the properties of a single particle or with the distribution of oxidation states of the particles suggests a potential way to characterize this distribution. We defer further considerations along these lines to future work and focus in this section on the size dependence aspect of the Fermi energy of a SC particle in equilibrium with an electrolyte solution. We stress that within the model approximations of the present work this equilibrium is completely determined by the solution of the Poisson–Boltzmann equation as described in section II and that the discussion in this section just gives another representation of this solution. In section II we have characterized the equilibrium state of the particle by its charge  $Q_{SC}$ , given that its Fermi energy is equal to that of the electrolyte. A more appealing description of the state of the SC particle would express its Fermi energy as a function of its geometrical characteristics (here its radius  $R$ ) and its charge  $Q_{SC}$ . This will be similar to the usual way of expressing the ionization potentials and electron affinities of metal clusters in vacuum as functions of their size and charge.<sup>1,2,25</sup>

Note that it is not a priori clear that such a description is useful for a SC particle in a redox solution. To express  $E_{F,SC}$  as a function of  $Q_{SC}$ ,  $R$ , and properties of the bulk semiconductor (e.g.,  $E_{F,SC}^0$ ) would mean that the effect of the electrolyte enters only in determining the equilibrium charge, while in effect the presence of the electrolyte contributes another energy term—the solvation energy of the charged particle. Still, in analogy with the electrolyte redox system, where for low ionic concentrations we find that  $\Phi_{ox/red}$  depends approximately only on the concentrations of the redox components themselves (eq 25) (the effect of other components of the solution enters via their effects on the activity coefficients which were taken to be 1 in eq 25), we may hope that the direct effect (beyond the effect on  $Q_{SC}$ ) of the electrolyte on  $E_{F,SC}$  will be small. Indeed we find below that  $E_{F,SC}$  may be expressed to a good approximation in terms of  $E_{F,SC}^0$ ,  $Q_{SC}$ , and  $R$ , and that its explicit dependence on the surrounding electrolyte is relatively small.

We have not been able to find a rigorous explicit expression for  $E_{F,SC}$  from the solution of the PB equation. We did find for an n-type SC (and we expect an analogous situation for a p-type SC) that under a broad range of conditions the following expression is satisfied to a very good approximation

$$E_{F,SC} = E_{F,SC}^0 + \frac{R}{L_{SC}} \alpha(R) kT \ln \left[ 1 - \frac{Q_{SC}}{Q_{SC,max}} \right] \quad (27)$$

(25) (a) Engel, E.; Perdew, J. P. *Phys. Rev.* **1991**, *B43*, 1331. (b) Seidi, M.; Spina, M. E.; Brack, M. In the Proceedings of The International Symposium on Small Particles and Clusters, to be published in *Z. Phys. D*. (c) Makov, G.; Nitzan, A. To be published.

**TABLE I:**  $\alpha(R)$  Calculated from the Linear Approximation Eq 31 and Numerically from the Slopes of the Lines in Figure 6<sup>a</sup>

$R/L_{SC}$	$C(R)_{eq\ 32}$	$\alpha(R)_{eq\ 31}$	$\alpha(R)_{pzc}$	$\alpha(R)_{c_{red}=c_{ox}}$
10.0	0.076	0.401	0.401	0.471
8.0	0.074	0.411	0.410	0.433
7.0	0.072	0.419	0.417	0.406
5.0	0.066	0.446	0.442	0.343
4.0	0.061	0.473	0.468	0.340
2.0	0.042	0.648	0.635	0.523
1.0	0.022	1.089	1.056	1.011
0.5	0.010	2.054		
0.1	0.001	10.02		10.04

<sup>a</sup> For the latter, two values are shown: at the point of zero charge (pzc) and at  $C_{ox} = C_{red}$ .

$E_{F,SC}^0$ , the Fermi energy of the bulk SC (or of the uncharged particle) is equivalent here to the standard redox potential of the ion pair in eq 25,  $Q_{SC,max}$  is the maximum positive charging possible for the particle, e.g., for an n-type SC under depletion conditions  $Q_{SC,max} = qN_D V$ .  $\alpha(R)$  is a constant which depends on  $R$  for small  $R$ , and becomes size independent as  $R \rightarrow \infty$ .

Equation 27 cannot be derived as a rigorous result from the PB equation; however, its linearized form

$$E_{F,SC} = E_{F,SC}^0 - \frac{R}{L_{SC}} \alpha(R) kT \frac{Q_{SC}}{Q_{SC,max}} \quad (28)$$

can be derived (using the charge conservation condition,  $Q_{SC} = -Q_{el}$ , and the continuity eqs 26) from the linearized PB equation, i.e., for situations characterized by small potential drop in the particle and in the electrolyte. This calculation yields

$$\alpha(R) = \frac{1}{1 - C(R)} \frac{(R/L_{SC})}{3 \left[ \frac{R}{L_{SC}} \coth \left( \frac{R}{L_{SC}} \right) - 1 \right]} \quad (29)$$

where

$$C(R) = \left[ 1 - \frac{L_{SC} \epsilon_{el} (L_{el} + R)}{L_{el} \epsilon_{SC} \left[ L_{SC} - R \coth \left( \frac{R}{L_{SC}} \right) \right] \left[ 1 + \frac{\epsilon_{el}}{4\pi c_H} \left( \frac{1}{R} + \frac{1}{L_{el}} \right) \right]} \right]^{-1} \quad (30)$$

When  $R \rightarrow \infty$ ,  $\alpha = (3(1 - C))^{-1}$ , where  $C$  is given by

$$C = \left[ 1 - \frac{\epsilon_{el} L_{SC}}{\epsilon_{SC} L_{el}} \frac{1}{1 + \epsilon_{el}/(4\pi c_H L_{el})} \right]^{-1} \quad (31)$$

Note that  $C(R)$  depends on  $L_{el}$  and  $\epsilon_{el}$ , and thus  $\alpha(R)$  is *not* a property of the SC only. The latter becomes approximately true if  $C(R) \ll 1$ . In particular this happens if the potential drop between the center of the particle and the bulk of the electrolyte occurs mostly in the particle. In Table I we show results for CdS particles in  $Mv^+/Mv^{2+}$  electrolyte solutions (parameters are the same as used in section II:  $L_{SC} = 252 \text{ \AA}$ ,  $c_{el} = c_{Mv^+} + c_{Mv^{2+}} = 1 \times 10^{17} \text{ ions/cm}^3$ , counterion charge =  $-2$ ,  $T = 300 \text{ K}$ ). For this system  $\alpha(\infty)$  is 0.365. It is seen that for this system  $C(R) \ll 1$  holds quite well.

The validity of eq 27 beyond the linear regime can be tested by calculating  $Q_{SC}$  for a SC particle at equilibrium with the electrolytic redox system (as was done in section II) and to plot  $\log(1 - Q_{SC}/Q_{SC,max})$  vs  $\log(c_{red}/c_{ox})$ . The latter quantity is proportional to  $E_{F,el}$  which is in turn equal to the equilibrium value of  $E_{F,SC}$ . Such a plot is shown in Figure 6 for a CdS particle in  $Mv^+/Mv^{2+}$  solution (with parameters for both systems as detailed above). The approximate linear relation between  $\log(1 -$

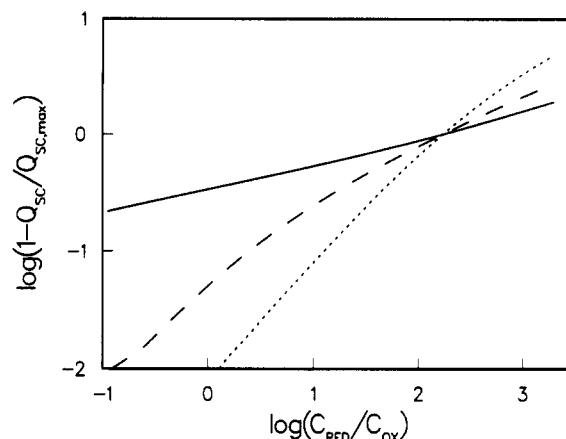


**Figure 6.**  $\log(1 - Q_{SC}/Q_{SC,max})$  plotted against  $\log(c_{red}/c_{ox})$  for a CdS particle in equilibrium with an electrolyte solution containing the  $Mv^+/Mv^{2+}$  redox system and a counterion of charge  $-2$ . Parameters for the CdS and for the electrolyte are given in the text. Full line, dashed line, and dotted line are for  $R/L_{SC} = 10, 5,$  and  $2,$  respectively. The point of zero charge is  $c_{red}/c_{ox} = 171.1$ , for which  $E_{F,el} = E_{F,SC}^0$ .

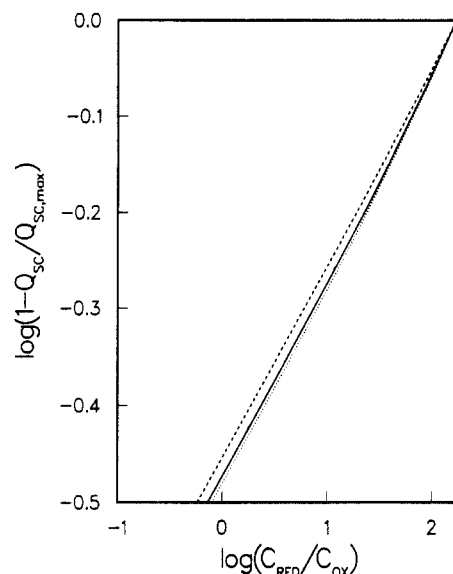


**Figure 7.** Same as Figure 6, for  $R/L_{SC} = 10$ , and for different electrolyte concentrations: dashed, full, and dotted lines correspond to  $c_{el} = c_{Mv^+} + c_{Mv^{2+}} = 10^{16}, 10^{17},$  and  $10^{18}$ , respectively. Only the depletion region is shown here.

$Q_{SC}/Q_{SC,max}$ ) and  $\log(c_{red}/c_{ox})$  confirms the approximate validity of eq 27. At the point of zero charge,  $Q_{SC} = 0$ , which for the present choice of parameters is obtained for  $c_{red}/c_{ox} = 171.1$ , all the lines in Figure 6 meet. Near this point the linearized PB equation holds, and  $\alpha(R)$  calculated from eq 29 is indeed equal to  $\alpha(R)$  obtained from the slope of the lines in Figure 6 at this point (see Table I). (Note that if  $a$  is the slope of a line in Figure 6,  $\alpha(R)$  is obtained from  $\alpha(R) = L_{SC}(Ra)^{-1}$ .) Far from the linear regime (e.g., the values given in Table I for the case  $c_{red}/c_{ox} = 1$ ) the  $\alpha(R)$  values are different, expressing the approximate nature of eq 27.

In Figure 7 we again plot  $\log(1 - Q_{SC}/Q_{SC,max})$  against  $\log(c_{red}/c_{ox})$  for  $R = 10L_{SC}$  and for the same parameters as in Figure 6, but now for different values of  $C_{el} = C_{red} + C_{ox}$ . If the relation 27 was independent of the electrolyte, these results should all fall on the same line. The small difference between the lines is another demonstration of the fact that the Fermi energy of the SC particle depends weakly on attributes of the electrolyte other than its redox potential.

The dependence of the relation between the particle's Fermi energy and its charge (eq 27) on the particle's size is expressed by the function  $\alpha(R)$ . This function is shown in Figure 8 for the system CdS/methylviologen, using the same parameters as in

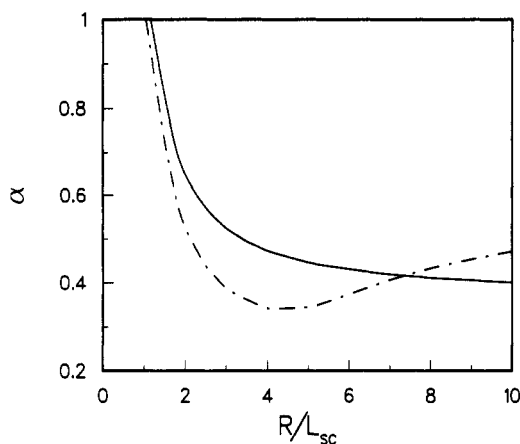


**Figure 8.** Function  $\alpha(R)$  (Table I) plotted against  $R/L_{SC}$  for CdS spheres in  $Mv^+/Mv^{2+}$  solution. Parameters for the CdS and for the redox system are given in the text. Full line: from the linearized PB equation (eq 31). Dashed line: from Figure 6 and Table I, for  $c_{red}/c_{ox} = 1$ .

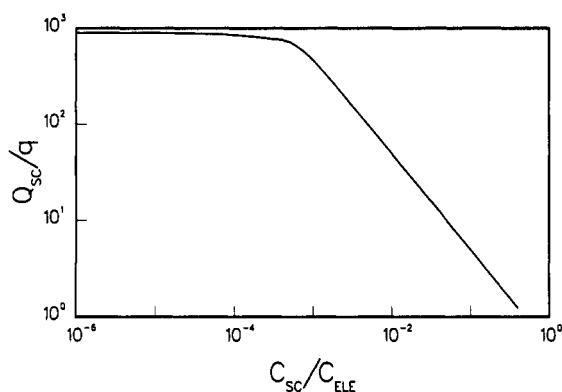


**Figure 9.** Equilibrium charge accumulated on a SC particle of size  $R = 10L_{SC}$  as a function of the ratio between the particle concentration and the electrolyte  $C_{ele} = C_{ox} + C_{red}$  concentration. The initial concentrations of the redox components are taken equal.

Figure 6 and in Table I. The full line represents the result based on the linear approximation, eq 29, and the dashed line corresponds to the  $\alpha(R)$  values obtained from the slopes of the lines in Figure 6 at the point  $c_{red}/c_{ox} = 1$ . Note that  $\alpha(R)$  becomes constant as  $R \rightarrow \infty$ . This results from the fact that in this limit  $Q_{SC}/Q_{SC,max} \sim 1/R$ , and  $E_{F,SC} - E_{F,SC}^0$  becomes simply the difference between the Fermi energies of the bulk electrolyte and the free macroscopic semiconductor. Note also that for  $R \rightarrow \infty$ , eq 28 is valid since  $Q/Q_{SC,max} \ll 1$ ; however,  $\alpha(R)$  is not necessarily given by eq 29 as seen in Figure 8.

So far we have studied a single SC particle in an infinite electrolyte solution. Next we consider a finite density of such particles.

#### IV. Colloidal Semiconductor Particles at Finite Density

Consider now a finite density  $c_{SC}$  of semiconductor particles, which for simplicity we take to be of uniform size, in equilibrium with an electrolyte redox system. We assume that the particle density is low enough so that direct interparticle interactions can be neglected. Therefore, the equilibrium state of each particle is determined by the surrounding electrolyte as was shown above. Unlike in the case of a single particle, the state of the electrolyte is now affected by the presence of the finite density of SC particles. In analogy to the equilibrium between chemical redox systems we may seek an "equilibrium constant" that will connect the system variables at equilibrium. Note that the analogy is not complete:

In the chemical case the system variables are only the concentrations, while in the present case the state of the semiconductor subsystem is determined by the concentration *and* the charge on the particles. When eqs 25 and 27 hold, this may be derived from

$$-q\Phi_{ox|red}^0 + \frac{kT}{n} \ln \frac{c_{red}}{c_{ox}} + C = E_{F,SC}^0 + \frac{R}{L_{SC}} \alpha(R) kT \ln \left[ 1 - \frac{Q_{SC}}{Q_{SC,max}} \right] \quad (32)$$

(note that  $c_{ox}$  and  $c_{red}$  represent in general products of concentrations). Taking for simplicity  $n = 1$  this leads to

$$\left[ 1 - Q_{SC}/Q_{SC,max} \right]^{R\alpha(R)/L_{SC}} (c_{ox}/c_{red}) = K(T) \quad (33)$$

$K(T)$  is the desired equilibrium constant. The dependence on  $Q_{SC}$  may be eliminated by using the charge conservation condition

$$c_{red} - c_{red}^0 = c_{ox}^0 - c_{ox} = (Q_{SC}/q)c_{SC} \quad (34)$$

Using this, eq 33 may be rewritten as

$$\left[ 1 + \frac{q(c_{ox} - c_{ox}^0)}{c_{SC}Q_{SC,max}} \right]^{R\alpha(R)/L_{SC}} \frac{c_{ox}}{c_{red}} = K(T) \quad (35)$$

In view of the remarks made following eq 27, this relation holds only approximately.

Finally, we note that eq 34 may be used to find the equilibrium values of  $Q_{SC}$ ,  $c_{ox}$ , and  $c_{red}$  in an equilibrium system formed by putting together the initial concentrations  $c_{ox}^0$ ,  $c_{red}^0$ , and  $c_{SC}$  of redox components and SC particles. This results from the fact that eq 34, together with the procedure used in section II to evaluate  $Q_{SC}$  in terms of  $c_{ox}$  and  $c_{red}$ , constitute a closed set of equations for these variables. In Figure 9 we show the result of such a calculation:  $Q_{SC}$  is plotted against  $C_{SC}/C_{ele}$ , where  $C_{ele} = C_{ox} + C_{red}$  for the case  $C_{ox}^0 = C_{red}^0$ . These results do not depend on the absolute values of  $C_{SC}$  and  $C_{ele}$ .

#### V. Conclusions

In this paper we have studied the equilibrium state in a solution containing an electrolytic redox pair and suspended colloidal SC particles. Similarities and differences between this and ordinary chemical equilibria are pointed out. Our calculations demonstrate the way in which the charging of the SC particle and its redox potential depend on the particle size and on the electronic properties of the bulk semiconductor. The charging changes its character from a volume effect to a surface effect as the particle size increases. The redox potential (Fermi energy) of the particle also depends on its size. We have obtained a useful, albeit approximate, relation (eq 27) between  $E_{F,SC}$  and the particle radius  $R$ . Consequently, the equilibrium constant of this system (e.g., eq 35) also depends on  $R$ . This size dependence can be strong for small particles and disappears as  $R \rightarrow \infty$ .

The model considered is simplified in many ways: The use of Poisson-Boltzmann statistics for the SC particles assumes both large enough particles, for which densities of impurities and carriers are meaningful concepts, and the unimportance of quantum effects. Also surface states on the SC particles are disregarded. The procedure used here can be carried over to models for which some of the present approximations (e.g., the absence of surface states) are relaxed.

**Acknowledgment.** This research was supported by the U.S.-Israel Binational Science Foundation and by the Israel Academy of Science. We thank Professor Joel Gersten for helpful discussions.

**Registry No.**  $MV^+$ , 25239-55-8;  $MV^{2+}$ , 4685-14-7; CdS, 1306-23-6.